

# Production of Primary Recrystallized Si-Fe Foil with Orientation near (110)[001] and Magnetic Properties

N. Abe, M. Iwasaki, K. Kosuge, Y. Ushigami, and T. Nozawa

The magnetic properties and features of magnetic domain structures of recently developed grain-oriented 15 to 50  $\mu\text{m}$  thick Si-Fe foil with very high permeability were investigated. The reported induction values of these materials were 1.70 to 1.95 T at 800 A/m. These high values produced low core losses. The losses of toroidal cores made of 50- $\mu\text{m}$  thick material was  $W_{15/400} = 8.0$  W/kg and  $W_{18/400} = 12.5$  W/kg. Despite the presence of a very small primary recrystallized grain size, they consisted of simple magnetic domains with  $180^\circ$  domain walls; ac magnetization was achieved by simple  $180^\circ$  domain wall displacement. The cut core, made of 20- $\mu\text{m}$  thick material, was  $W_{10/10k} = 330$  W/kg and  $W_{15/10k} = 580$  W/kg, which compares to those of amorphous cut cores.

## Keywords

core loss, cut core, foil, magnetic materials, Si-Fe foil

## 1. Introduction

LINE frequency loss has been improved primarily by improving crystal orientation and decreasing anomalous eddy current loss by increasing the number of effective  $180^\circ$  domain walls. On the other hand, these thick materials are not suitable for higher frequency magnetic applications because of higher eddy current density. Thin (110)[001] grain-oriented Si-Fe foil is required for high-frequency electrical apparatus. Particularly low core losses and high permeabilities at higher design flux densities and higher excitation frequencies greater than 400 Hz are necessary.

In 1949, Littmann studied noninhibitor processes for developing Si-Fe foil.<sup>[1]</sup> During his studies, when a material initially oriented in the (110)[001] fashion (permeability of 1740 at 800 A/m), having a satisfactory large grain size (grain diameter of from 0.05 to 10 mm), was subsequently cold rolled and recrystallized, permeabilities at 800 A/m were 1600 to 1700 at thicknesses of 25 to 125  $\mu\text{m}$ , and core losses were high particularly at high excitation levels.

The purpose of this article is to present the newly developed Si-Fe foil with low core loss at high design inductions for high-frequency applications,<sup>[2]</sup> as well as their magnetic properties and characteristics of domain wall behavior. Additionally, an attempt has been made to manufacture the cut core and compare the core loss with that of amorphous cut cores.

## 2. Experimental

### 2.1 Production of Very Highly (110)[001] Grain-Oriented Si-Fe

Many studies of cold rolling and primary recrystallization<sup>[2,3]</sup> indicated that, if starting materials have a sharp (110)[001] orientation, it is possible to produce sharp (110)[001] oriented Si-Fe foil. The grain boundaries of the starting material affect the cold rolled recrystallization texture. Grains with  $\{110\}\langle 001 \rangle$  type orientation nucleate at starting material grains and grow. On the other hand, grains with (111)[011] type orientation occur in the vicinity of old grain boundaries of the starting material.

Figure 1 shows the etch pits of Si-Fe foil. The (100) grains appear in grains and the (111) grains appear near the grain boundaries of the starting materials. According to these experimental facts, selection of starting materials with both ideal (110)[001] oriented grains and less grain boundary area is significant.

This unique starting material, in the form of a 5-ton coil, was developed by temperature-gradient secondary recrystallization annealing using a special furnace.<sup>[4]</sup> Figure 2 shows a portion of the macrostructure of this strip, and Fig. 3 shows the dc hys-

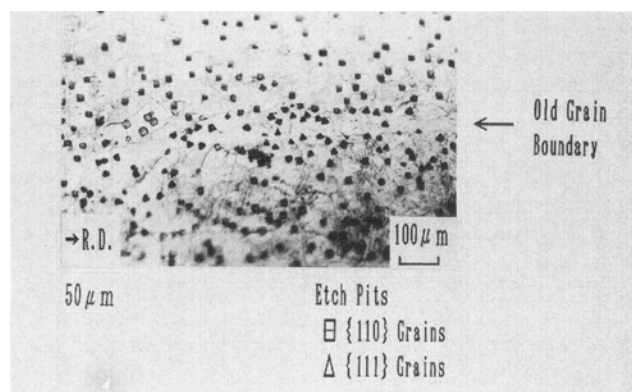
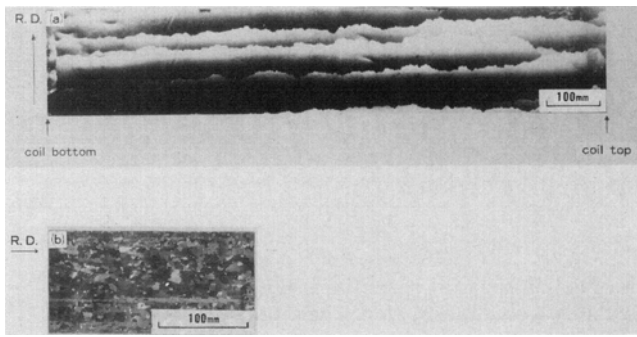
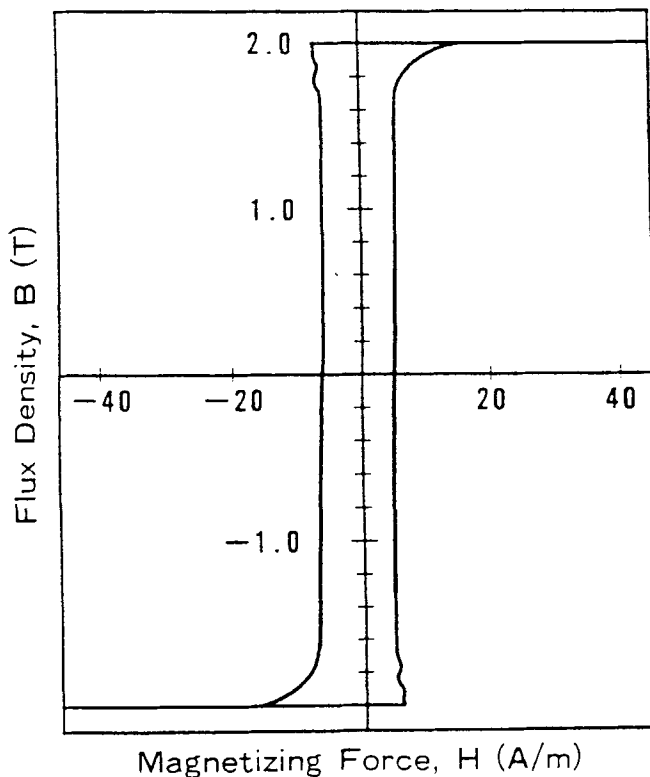


Fig. 1 Etch pits in Si-Fe foil.

N. Abe, M. Iwasaki, and K. Kosuge, Hirohata R&D Lab., Nippon Steel Corp., Himeji, Hyogo, Japan; and Y. Ushigami and T. Nozawa, Steel Research Labs., Nippon Steel Corp., Futaba, Chiba, Japan.



**Fig. 2** Macrostructure of grain-oriented 3Si-Fe strip. (a) Starting material of large grain diameter ( $40 \times 1000$  mm) and high  $B_8$  (2.00 T). (b) Starting material of small grain diameter ( $3 \times 5$  mm) and low  $B_8$  (1.85 T).



**Fig. 3** dc hysteresis loop of the starting material with large grain diameter ( $40 \times 1000$  mm) and high  $B_8$  (2.00 T).

teresis loop of this material. The maximum permeability is about 250,000. The perfect squareness ratio,  $B_r/B_s = 1.0$ , and reentrant shape hysteresis loop correspond to the ideal (110)[001] orientation and a very simple domain structure of  $180^\circ$  domain walls.

## 2.2 Production of Si-Fe Foil with Orientation near (110)[001]

The starting materials ( $B_8 = 1.98$  T, grain size =  $40 \times 1000$  mm, thickness = 150 to 200  $\mu\text{m}$ ) were cold rolled using a

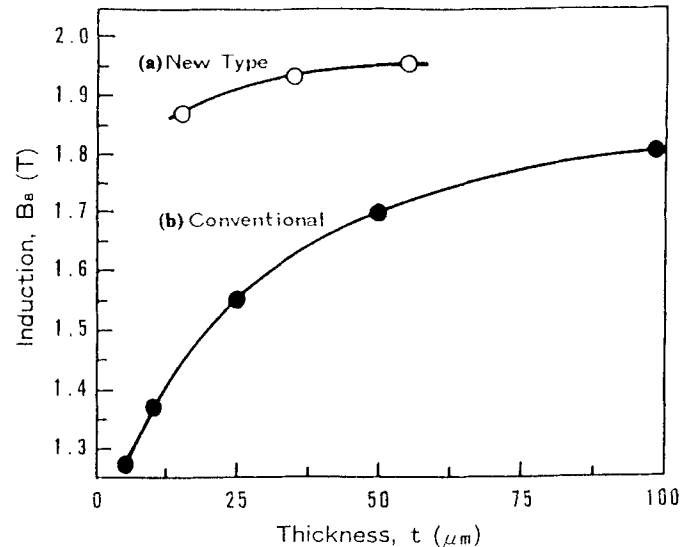


**Fig. 4** Relationship between induction  $B_8$  of primary recrystallized 3Si-Fe foil and sheet thickness. (a) Starting material of large grain diameter ( $40 \times 1000$  mm) and high  $B_8$  (2.00 T). (b) Starting material of small grain diameter ( $3 \times 5$  mm) and low  $B_8$  (1.85 T).

sendzimir mill with 18 back-up rolls and a 10.5-mm diameter work roll to a final thickness of 15 to 50  $\mu\text{m}$ . Specimens were then annealed at 800 to 1000  $^\circ\text{C}$  for 30 to 600 s in a hydrogen atmosphere, followed by annealing in a nitrogen atmosphere to form insulating films.

Tape-wound toroids of Si-Fe foil were stress relief annealed. Some of these toroids were laser irradiated after stress relief annealing.

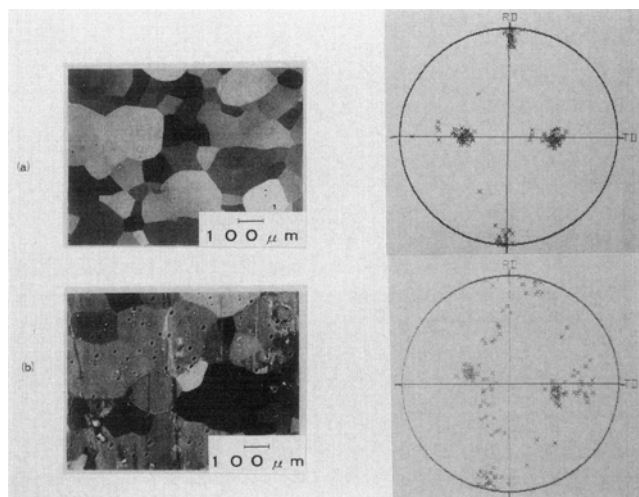
The domain patterns were observed using high-voltage scanning electron microscopy (SEM). Dynamic domain wall behavior was observed using a newly developed SEM line-sampling stroboscopic method.<sup>[5]</sup>

## 3. Results and Discussion

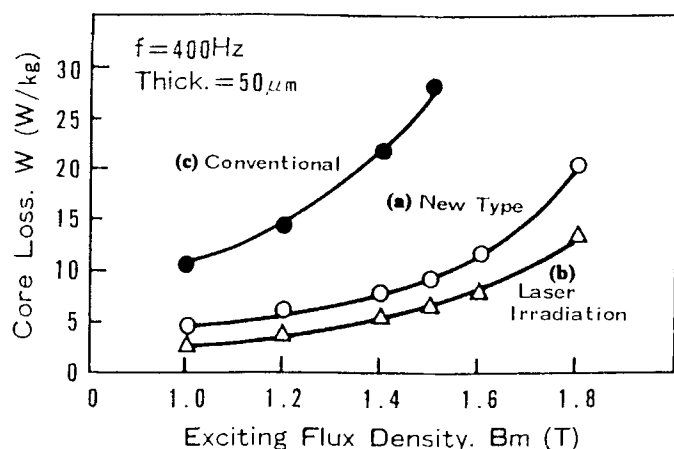
Figure 4 shows the relationship between induction,  $B_8$ , of primary recrystallized foil and foil thickness. The  $B_8$  values of the foil strongly depend on two variables—the  $B_8$  value and grain size of the starting material.

Figure 5 shows grain structures for foils and crystal orientations of each grain determined by the electron channeling pattern method. This figure shows that the crystal orientations of primary recrystallized foil made from highly grain-oriented large grain starting material are near (110)[001].

Figure 6 shows the relationship between core loss at  $f = 400$  Hz and the maximum exciting flux densities. The core losses are  $W_{15/400} = 9$  W/kg and  $W_{18/400} = 22$  W/kg. After laser irradiation, the losses decrease to 8 W/kg and 14 W/kg, respectively. These values are about 40% lower than those of conventional materials. These very low losses at higher inductions are a distinct feature of highly oriented (110)[001] Si-Fe foil. The decrease in core loss caused by use of laser irradiation



**Fig. 5** Grain structures for Si-Fe foil and crystal orientations of each grain determined by the electron channeling pattern method. (a) Grain structures. (b) Crystal orientations of each grain.

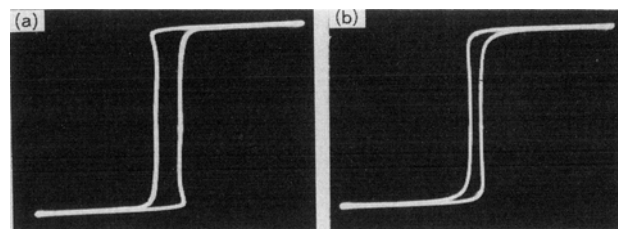


**Fig. 6** Relationship between core loss of Si-Fe foil toroidal core at  $f = 400$  Hz and maximum exciting flux density. (a) Starting material of large grain diameter ( $40 \times 1000$  mm) and high  $B_8$  (2.00 T).  $B_8$  of Si-Fe foil is 1.95 T. (b) After laser irradiation of (a). (c) Starting material of small grain diameter ( $3 \times 5$  mm) and low  $B_8$  (1.85 T).  $B_8$  of Si-Fe foil is 1.60 T.

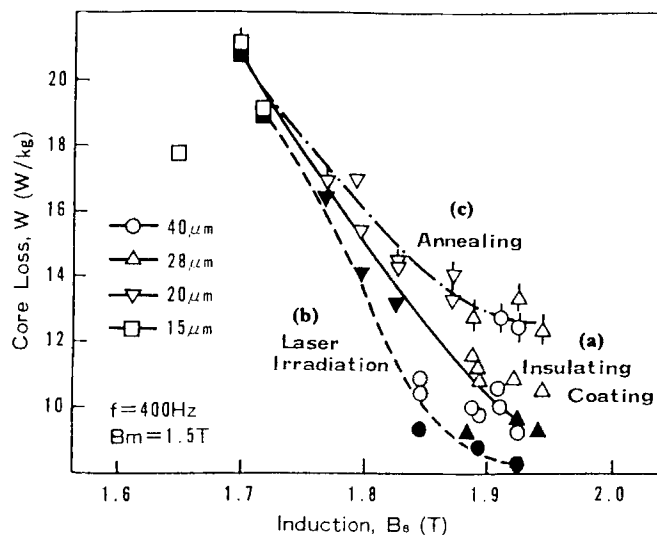
is due to an increase in the number of effective domain walls (see Fig. 9).

Figure 7 shows the hysteresis loop at 400 Hz magnetization. The loop shape change (resembling a snake-like pattern) corresponds to an increase in the number of domain walls that contribute to reverse magnetization (see Fig. 9).

Figure 8 illustrates the dependence of decreasing core loss on  $B_8$  as a function of isotropic tensile stress (coating) and local stress (laser irradiation) in material of various thicknesses. This figure shows that the losses at 400 Hz do not depend on thickness, but primarily on  $B_8$  value. The decrease in loss in higher  $B_8$  materials is due primarily to the domain wall spacing refining effect (see Fig. 9 and 10).



**Fig. 7** Hysteresis loop at  $f = 400$  Hz magnetization of Si-Fe foil. (a) Before laser irradiation. (b) After laser irradiation.



**Fig. 8** Induction  $B_8$  dependence of loss decreasing effect due to isotropic tensile stress (coating) and local stress (laser irradiation). (a) Before laser irradiation with coating. (b) After laser irradiation with coating. (c) Before laser irradiation with no coating.

On the other hand, the ineffectiveness in lower  $B_8$  material can be attributed to a local stress and a magnetostatic defect induced at grain boundaries based on the large variation of crystal orientation from grain to grain.

Figures 9 and 10 illustrate the domain patterns of Si-Fe foil. Despite the small grains (see Fig. 4), they consist of large slab-like domains. Using laser irradiation decreases the main domain wall spacings to about one tenth. The striped patterns near the laser spots are supplemental domains with transverse magnetization. There are many fine spots in the main domains. They are supplemental domains caused by demagnetizing fields near grain boundaries and/or tilting of the [001] component out of the sheet plane. In poorly grain-oriented material, the magnetic domain images generally are not clear. Narrow, snaky domains, like the growth rings of a tree, are observed. The main domain wall spacings of Si-Fe foil are refined, largely due to isotropic tensile stress due to surface coating (see Fig. 10).

Figure 11 shows the dynamic domain patterns corresponding to each phase during ac magnetization. These patterns illustrate that the magnetization of highly grain-oriented Si-Fe foil is achieved mainly by  $180^\circ$  domain wall displacement. On the

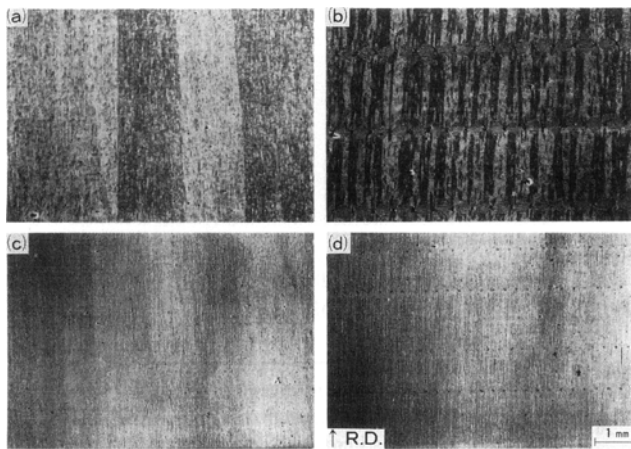


**Fig. 9** Demagnetized domain patterns of Si-Fe foil. (a) Starting material of large grain diameter ( $40 \times 1000$  mm) and high  $B_g$  (2.00 T).  $B_g$  of Si-Fe foil is 1.95 T. (b) After laser irradiation of (a). (c) Starting material of small grain diameter ( $3 \times 5$  mm) and low  $B_g$  (1.85 T).  $B_g$  of Si-Fe foil is 1.60 T. (d) After laser irradiation of (c).

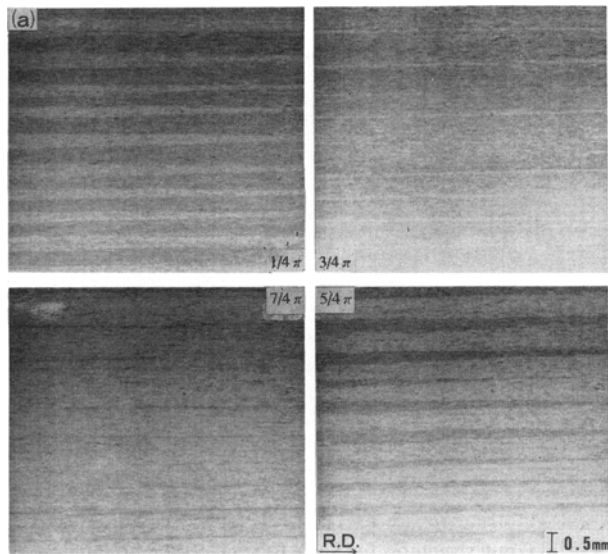


**Fig. 10** Demagnetized domain patterns of Si-Fe foil. (a) Starting material of large grain diameter ( $40 \times 1000$  mm) and high  $B_g$  (2.00 T).  $B_g$  of Si-Fe foil is 1.95 T. (b) After coating of (a). (c) Starting material of small grain diameter ( $3 \times 5$  mm) and low  $B_g$  (1.85 T).  $B_g$  of Si-Fe foil is 1.60 T. (d) After coating of (c).

other hand, the wall behavior in lower  $B_g$  material is not uniform. These figures suggest that domain wall velocities change from place to place. Furthermore, low magnetic domain image contrast implies that the magnetization is achieved by low reproducible main wall behavior and/or rearrangement of supplementary domains during dc magnetization.

Figure 12 shows the relationship between core loss per frequency and the frequency at various thicknesses. The linear core loss increase up to about 5 kHz suggests that magnetization is achieved by simple main domain wall displacement similar to dynamic domain wall behavior at 50 Hz magnetiza-

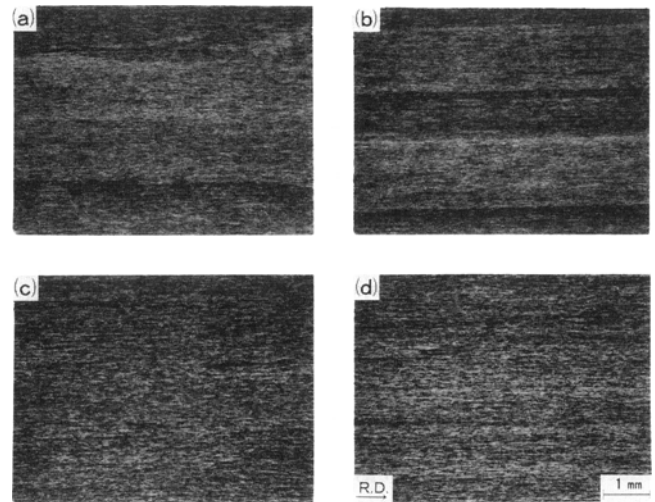


**Fig. 11(a)** Dynamic domain patterns corresponding to each phase during ac magnetization in higher  $B_g$  material before laser irradiation with coating. Starting material of large grain diameter ( $40 \times 1000$  mm) and high  $B_g$  (2.00 T).  $B_g$  of Si-Fe foil is 1.95 T.

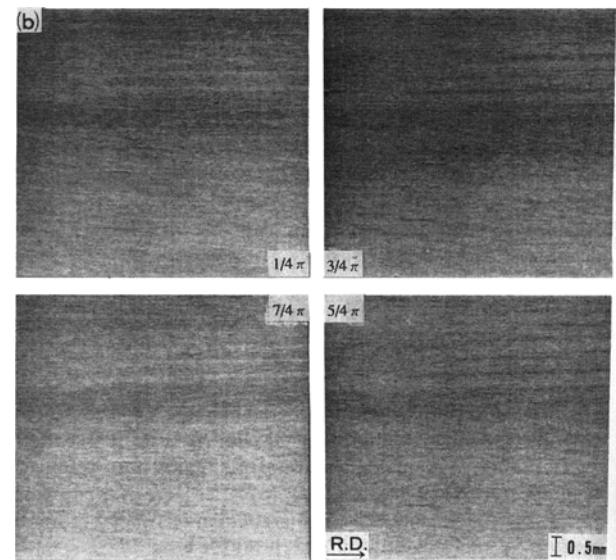


**Fig. 11(b)** Dynamic domain patterns corresponding to each phase during ac magnetization in higher  $B_g$  material before laser irradiation with coating. Starting material of small grain diameter ( $3 \times 5$  mm) and low  $B_g$  (1.85 T).  $B_g$  of Si-Fe foil is 1.60 T.

tion. The rapid increase in core loss at more than 5 kHz reflects the changes in the magnetization processes. At 10,000 Hz, the low core loss does not only depend on  $B_g$  values, but also on sheet thickness, as can be seen by comparing to Si-Fe foils with thickness of 40 and 28  $\mu\text{m}$ , which have the same  $B_g$  values. The lowest core loss at 10,000 Hz is 480 W/kg using laser-irradiated Si-Fe foil with a thickness of 28  $\mu\text{m}$ . Therefore, to achieve low core loss, high  $B_g$  values and many domain walls are needed.

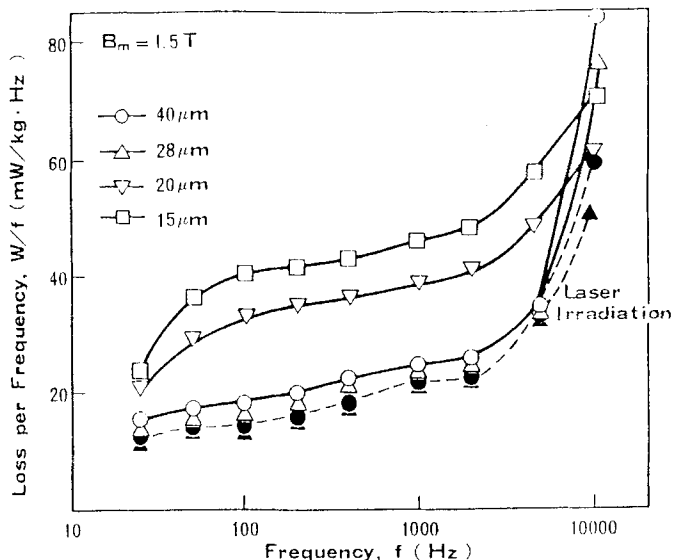


Fig. 12 Relationship between core loss per frequency and frequency.

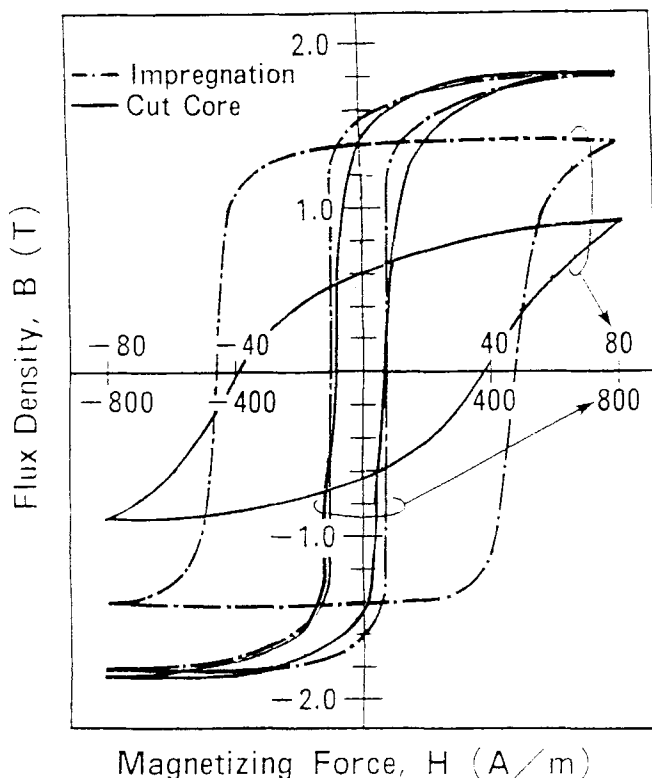


Fig. 13 dc hysteresis loop of the impregnation core (non-cut core) and the cut core.

Figure 13 shows the dc hysteresis loop of the impregnation core and cut core. In spite of impregnation, the shape of the dc hysteresis loop does not change. However, after cutting, the shape became inclined, and coercive forces decreased slightly,

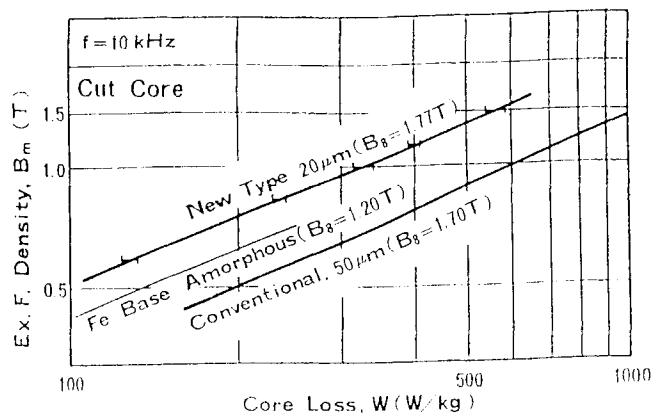


Fig. 14 Relationship between core loss of Si-Fe cut core at  $f = 10$  kHz and maximum exciting flux density.

most likely because stress introduced by impregnation was relieved by cutting.

Figure 14 shows the relationship between core loss at 10 kHz and exciting flux density. The new type of cut core can be used at densities above 1.0 T, and the core loss compares with those of Fe-Si-B amorphous cut cores. The core loss at 1.0 T was 330 W/kg and at 1.5 T it was 580 W/kg.

#### 4. Conclusions

Grain-oriented Si-Fe foil with orientation near (110)[001] has been developed recently. By refining of main domain wall spacing due to isotropic tensile stress and/or periodically induced local stresses, core losses decreased significantly. Core losses of these materials at middle frequencies were low, particularly at higher inductions. Although very small in grain size, they are composed of simple domains, and ac magnetization up to about 5 kHz is achieved by simple 180° main domain wall displacement.

The core losses of cut cores compare with those of Fe-Si-B amorphous cut cores at 10 kHz. The present results were 330 W/kg at 1.0 T and 580 W/kg at 1.5 T. These materials are useful for transformers and/or inductors for middle frequencies and higher design induction applications.

#### Acknowledgment

The authors wish to thank Mr. H. Mogi for his help in observing domain patterns.

#### References

1. M.F. Littmann, US patent No. 2,473,156
2. N. Abe, Y. Ushigami, M. Iwasaki, and T. Nozawa, 14th Ann. Conf. on Magnetism in Japan, The Magnetism Society of Japan, Matsuyama C., Japan, 1990, p 402
3. T. Taoka, *Tetsu Hagane*, Vol 54 (No. 2), 1968, p 22
4. T. Nozawa, T. Nakayama, Y. Ushigami, and T. Yamamoto, *J. Magn. Magn. Mater.*, Vol 58, 1986, p 67-77
5. H. Mogi, M. Yabumoto, Y. Matsuo, and K. Koyanagi, to be published, 1993